

# Optimization Design and Research of Injection Molding Process of Raspberry + Pi+2+ Shell

Dengping Hu<sup>1</sup>, Qian Leng<sup>2,\*</sup>, Dandan Wang<sup>3</sup>, Longwei Zhong<sup>1</sup>, Zesi Yao<sup>1</sup>, Han Zhang<sup>1</sup>

<sup>1</sup>Sino-German College of Intelligent Manufacturing, Shenzhen Technology University, Shenzhen, Guangdong, China

<sup>2</sup>Faculty of Engineering, The Hong Kong Polytechnic University, Hong Kong, China

<sup>3</sup>School of Foreign Studies, Guangzhou University, Guangzhou, Guangdong, China

\*Corresponding Author

**Abstract:** Raspberry Pi+ Pi+2+ shell is composed of a typical plate shell appearance plastic body, which is a thin-walled plastic part with holes. When the surface size of the plastic part changes during injection molding, it is easy to warpage deformation, which seriously affects the surface quality and assembly accuracy of the plastic part. In order to make the product more appropriate to the actual engineering results, this study uses a solid grid with higher calculation accuracy to simulate it. In order to improve cooling efficiency, the Raspberry Pi shell is cooled using a partition water channel and a form-following cooling channel. Using Moldflow software, the injection molding process of a thin-walled Raspberry Pi shell was simulated and analyzed. An orthogonal test table with 4 factors and 4 levels was designed, and 16 simulation analysis experiments were conducted on it. Pearson correlation analysis and range analysis in mathematical analysis methods were used to screen important influences and select the best injection molding scheme. The results show that the degree of influence of each factor on warping deformation is holding pressure > holding pressure time > cooling time > melt temperature. The optimal process parameters are A1B4C4D4, that is, the melt temperature is 200°C, the holding pressure is 60MPa, the holding time is 14s, and the cooling time is 22s. The maximum warpage deformation decreased from 0.8515mm before optimization to 0.6939mm after optimization, with a decrease of about 18.5%. Because the Raspberry PI is loaded with extremely small high-precision components, the dimensional tolerance assigned to each precision component will be reduced by one precision level, and the

precision of the detection and control of precision components will be a qualitative leap.

**Keywords:** Raspberry Pi Shell; Thin-Walled Parts; Bulkhead Waterway; Form-Following Cooling Taguchi Test; Warping Deformation Optimization

## 1. Introduction

Miniature computers, roughly the size of a credit card, are equipped with a variety of hardware interfaces and can support any ARM-based operating system, such as certain Linux distributions, Android, and Windows IoT. These devices are versatile and can be used in scenarios such as personal computers, servers, multimedia terminals, and IoT devices.

However, the official casing of a particular miniature computer has certain design shortcomings: the process of replacing the SD card is cumbersome and complicated; the placeholder holes on the casing's fake stand serve no functional purpose; and the device's operating temperature may rise excessively. Plastic plays an important role in the manufacturing industry today. Many plastic manufacturing processes are available such as blow molding, casting, compression molding, extrusion, fabrication, foaming, injection molding, rotational molding, and thermoforming<sup>[1]</sup>. In recent years, mold flow analysis—a finite element simulation technique using CAE software to analyze processes like injection, packing, cooling, and warping of plastic parts—was initially used only for diagnosing issues in plastic product design and aiding in production problem-solving<sup>[2]</sup>. However, with technological advancements, mold flow analysis has been widely adopted in the industry for early-stage design, verification,

and optimization of products and molds, playing a vital role in the design and manufacturing processes of most enterprises<sup>[3]</sup>. The process of injection molding is a widely used method of manufacturing plastic materials on an industrial scale, capable of producing objects of various sizes and shapes, including complex ones, with a high level of efficiency<sup>[4]</sup>. The products are made from polymers that have different behaviors depending on the type of monomer<sup>[5]</sup>.

With the progress in computer-aided engineering simulation tools, such as the widely used Moldflow in the injection molding industry, engineers could evaluate the flow patterns of polymer melts during injection, packing, and cooling inside the molds<sup>[6]</sup>. In the Moldflow program from Autodesk, there is already a crystallization kinetic consideration for semi crystalline plastics, which includes the influence of the cooling rate in the crystallization, but this function can only be used for a middle layer or surface meshed parts and is therefore unsuitable for complex geometries<sup>[7]</sup>. Till date, most of the studies suggest that the output of plastic injection molding process is largely dependent upon operator's skills and optimum process parameters<sup>[8]</sup>. Higher melt and mold temperatures, as well as higher injection speeds (shear), increase melt flow, which improves precision<sup>[9]</sup>. Autodesk Moldflow Insight is a useful software that can simulate rheological behavior and thermal conditions of polymers during injection molding with the help of the finite element method and subsequently elucidate the effect of material and operational parameters on final product quality<sup>[10]</sup>. G. Singh et al. <sup>[11]</sup> find that most researchers believe that Moldflow Plastic Insight software generated simulation analysis reports gave good results in comparison to any other software.

In this study, the official casing of a particular miniature computer was selected as the research object. Appropriate material selection, mesh type, gate location, and cooling strategies were determined, and Moldflow software was used to simulate the injection molding process of the thin-walled miniature computer casing. Cooling and warping analysis results were obtained, followed by 16 simulation experiments. The key influencing factors were identified using mathematical analysis

techniques such as Pearson correlation analysis and range analysis in SPSSPRO software, and the optimal injection molding scheme was determined. This provides a reference for the theoretical and high-precision development of injection molding for miniature computer casings.

## 2. Miniature Computer Casing and Material Properties

The physical structure of the miniature computer casing is shown in Figure 1a, where the red casing represents the upper shell of the miniature computer, and the gray casing represents the lower shell. Due to the greater structural complexity of the upper shell compared to the lower shell, as well as higher surface quality requirements, defects such as sink marks and warping are not permissible. This study focuses primarily on the optimization design of the injection molding process for the upper shell of the miniature computer.

The structure of the upper casing is illustrated in Figure 1a. The overall dimensions of the product are 90.6 mm × 62 mm × 12.5 mm, with a wall thickness of 2 mm. The casing was reverse-engineered and modeled, resulting in the computer casing model shown in Figure 1b.

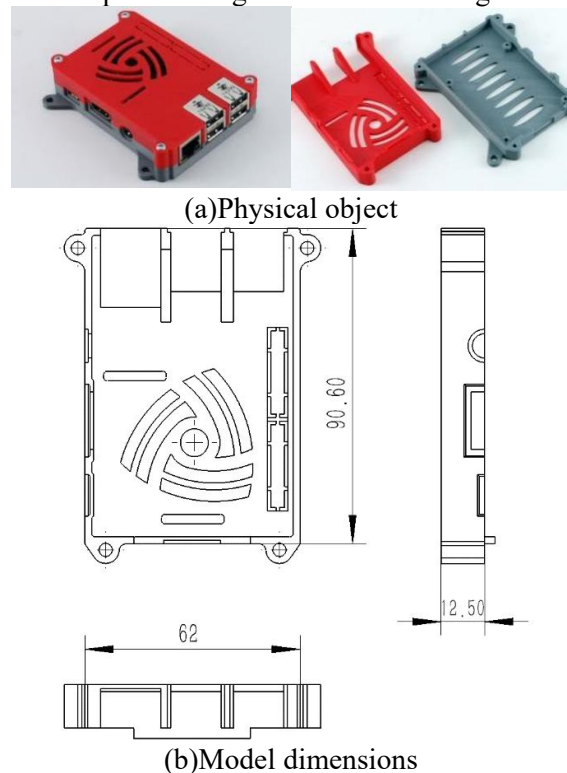


**Figure 1. Miniature Computer Casing Model**

The material selected for the study is polypropylene (PP), specifically the grade POLYLAM RIPP 3625 CS1. Polypropylene (PP) is a widely used thermoplastic polymer known for its versatility, durability, and ease of processing. It is produced through the polymerization of propylene monomers and is characterized by its high chemical resistance, low moisture absorption, and relatively low density, making it an ideal material for a range of applications. Polypropylene exhibits good mechanical strength and excellent resistance to fatigue, which makes it suitable for products that undergo repeated stress. It is commonly used in industries such as packaging, automotive, textiles, and consumer goods, as well as in medical and industrial applications. PP can be molded into a variety of shapes and forms, and it is often chosen for its cost-effectiveness and environmental benefits, as it can be recycled easily.

The recommended processing temperature range for this material is 180–260°C, with a mold temperature range of 20–80°C. The recommended injection molding process parameters include: mold surface temperature of 50°C, melt temperature of 220°C, mold temperature range of 20–80°C, melt temperature range of 180–260°C, an absolute maximum melt temperature of 300°C, and an ejection temperature of 124°C.

### 3. Moldflow Simulation and Mold Structure Optimization

#### 3.1 Gating and Cooling System Design

The miniature computer casing qualifies as a small, thin-walled injection-molded part. Considering the casing's dimensions and its thin-walled characteristics, a multi-cavity mold design was selected for the injection molding process<sup>[12]</sup>. However, increasing the number of cavities does not always yield better results, as manufacturing multi-cavity molds can be expensive and may significantly raise production costs. Therefore, taking into account mold cost, production efficiency, and utilization rate, a two-cavity mold design was chosen for the injection molding of the miniature computer casing<sup>[13]</sup>.

During the product design phase, lightweight design principles and heat dissipation requirements for the miniature computer were considered. Internal ribs were removed to

reduce weight. For thin-walled containers with through-holes, the gate location should avoid areas with hollowed ribs whenever possible<sup>[14]</sup>. From the gate location analysis cloud map in Figure 2, it is evident that the gate performs best when placed in the central region, achieving optimal compatibility.

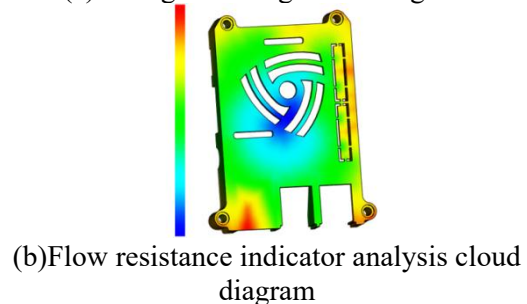
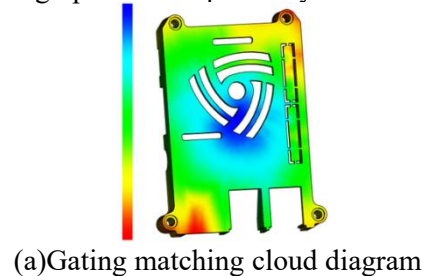


**Figure 2. Gating Position Analysis Cloud Diagram**

Based on the above principles, the designed gating and cooling system is illustrated in Figure 3. Conformal cooling is employed externally, while the internal walls are cooled using a cooling water channel with baffles.

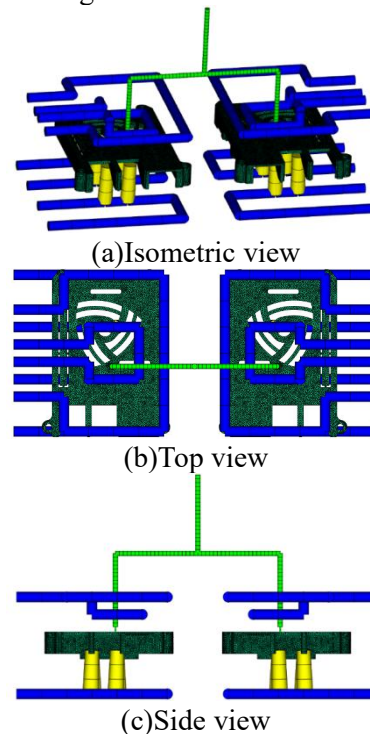


**Figure 3. Cooling Water Channels**

### 3.2 Cooling Analysis

As shown in Figures 4a and 4b, the baffle cooling channels and conformal cooling circuits are well-designed. With a cooling fluid temperature of 25°C, the part is able to maintain a temperature close to 25°C after cooling.

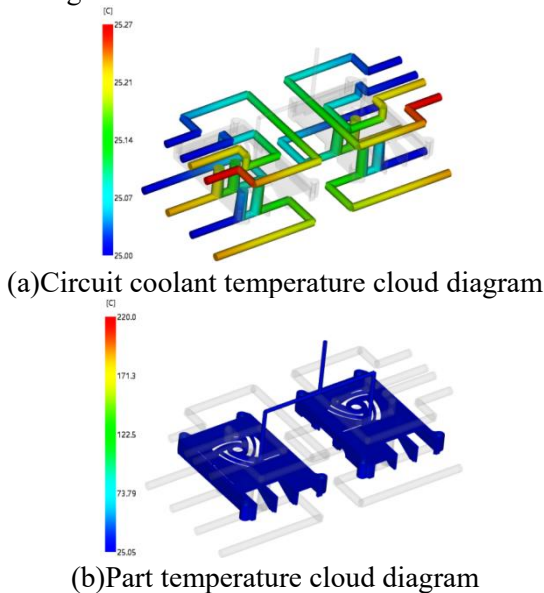


**Figure 4. Cooling Analysis Results**

### 2.3 Warpage Analysis

As shown in Figure 5, an analysis conducted using the recommended parameters revealed that the maximum warpage deformation of the miniature computer casing is 0.8515 mm. Since the casing houses precision components with high dimensional accuracy, its internal structure must remain stable with no significant gaps. This ensures that the internal precision components will not experience relative displacement due to minor vibrations during operation. A warpage deformation of 0.8515 mm is unacceptable. Considering the number of internal components and their dimensional tolerances, the maximum allowable warpage margin is now limited to 0.7 mm.

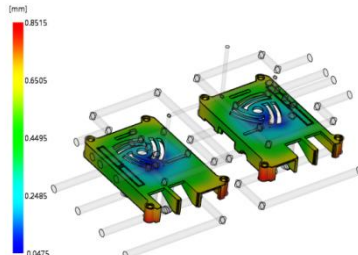


**Figure 5. Warpage Deformation Cloud Diagram**

## 4. Molding Process Parameter Optimization Analysis

### 4.1 Taguchi Orthogonal Experiment Design

The Taguchi method is widely applied in multi-criteria decision-making due to its ability to save time and resources. It uses orthogonal arrays to design experimental plans and conduct computational analyses, enabling the acquisition of accurate data and results with fewer experimental trials. By considering the effects of factors on variability, this method enhances the stability and reliability of product design<sup>[15]</sup>.

In this study, the total warpage deformation was selected as the evaluation target, with melt temperature (A), holding pressure (B), holding time (C), and cooling time (D) as the primary variables for analysis. Initial process parameters were set based on the CAE analysis results, material properties, and the recommended values from the Moldflow software material database. A 4-factor, 4-level orthogonal experimental design was adopted, and the levels of the selected factors are shown in Table 1.

**Table 1. Warpage Deformation Range Analysis**

| Levels | Factors |       |     |     |
|--------|---------|-------|-----|-----|
|        | A/°C    | B/MPa | C/s | D/s |
| 1      | 200     | 30    | 8   | 16  |
| 2      | 210     | 40    | 10  | 18  |
| 3      | 220     | 50    | 12  | 20  |
| 4      | 230     | 60    | 14  | 22  |

### 4.2 Taguchi Orthogonal Experiment Results

Based on Table 1, 16 simulation experiments were conducted. The experimental plan, with the 4 parameters and 4 levels, along with the experimental results, are summarized in Table 2.

**Table 2. Orthogonal Experiment Plan and Result Data**

| Experiment Number | A/°C | B/Mpa | C/s | D/s | Total Warpage Deformation/mm |
|-------------------|------|-------|-----|-----|------------------------------|
| 1                 | 200  | 30    | 8   | 16  | 0.7673                       |
| 2                 | 200  | 40    | 10  | 18  | 0.7368                       |
| 3                 | 200  | 50    | 12  | 20  | 0.712                        |
| 4                 | 200  | 60    | 14  | 22  | 0.712                        |
| 5                 | 210  | 30    | 8   | 16  | 0.808                        |
| 6                 | 210  | 40    | 10  | 18  | 0.7556                       |
| 7                 | 210  | 50    | 12  | 20  | 0.7243                       |
| 8                 | 210  | 60    | 14  | 22  | 0.7069                       |
| 9                 | 220  | 30    | 8   | 16  | 0.8155                       |

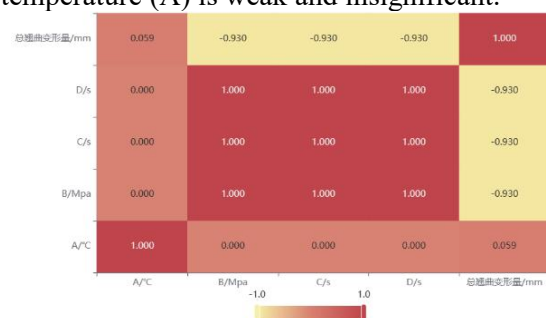
|    |     |    |    |    |        |
|----|-----|----|----|----|--------|
| 10 | 220 | 40 | 10 | 18 | 0.7559 |
| 11 | 220 | 50 | 12 | 20 | 0.7242 |
| 12 | 220 | 60 | 14 | 22 | 0.7021 |
| 13 | 230 | 30 | 8  | 16 | 0.7997 |
| 14 | 230 | 40 | 10 | 18 | 0.7468 |
| 15 | 230 | 50 | 12 | 20 | 0.7151 |
| 16 | 230 | 60 | 14 | 22 | 0.6918 |

**Table 3. Pearson Correlation Analysis Results**

|                              | A/°C         | B/Mpa           | C/s             | D/s             | Total Warpage Deformation/mm |
|------------------------------|--------------|-----------------|-----------------|-----------------|------------------------------|
| Total Warpage Deformation/mm | 0.059(0.830) | -0.93(0.000***) | -0.93(0.000***) | -0.93(0.000***) | 1(0.000***)                  |

Note: \*\*\* \*\*, and \* represent significance levels of 1%, 5%, and 10%, respectively.

Table 3 and Figure 6 presents the results of the Pearson correlation analysis, examining the relationships between variables A (temperature/°C), B (pressure/Mpa), C (time/s), D (time/s), and the total warpage deformation (mm). The correlation coefficient between total warpage deformation and temperature (A) is 0.059, with a p-value of 0.830, indicating a very weak and statistically insignificant correlation. The correlation coefficient between total warpage deformation and pressure (B) is -0.93, with a p-value of 0.000\*\*\*, indicating a strong negative correlation that is highly significant at the 1% level. Similarly, the correlation coefficient between total warpage deformation and time C is -0.93, with a p-value of 0.000\*\*\*, also indicating a strong negative correlation that is highly significant at the 1% level. The correlation coefficient between total warpage deformation and time D is -0.93, with a p-value of 0.000\*\*\*, again showing a strong negative correlation that is highly significant at the 1% level. The correlation coefficient of total warpage deformation with itself is 1, with a p-value of 0.000\*\*\*, representing a perfect positive autocorrelation. In summary, pressure (B) and time (C, D) are key factors influencing total warpage deformation, with highly significant correlations, while the effect of temperature (A) is weak and insignificant.

**Figure 6. Pearson Correlation Analysis Heatmap**

### 4.3 Warpage Deformation Correlation Analysis

Pearson correlation analysis of warpage deformation and its variables was performed using SPSSPRO software, and the following analysis results were obtained:

### 4.4 Warpage Deformation Results Analysis

All the total warpage deformation data for the factors were collected and subjected to range analysis. SPSSPRO software was used to perform the range analysis on the data from Table 2, and the results are shown in Table 3. Through range analysis, the influence of each factor and its respective levels on the indicator was determined.

**Table 4. Warpage Deformation Range Analysis**

|    | A     | B     | C     | D     |
|----|-------|-------|-------|-------|
| K1 | 2.928 | 3.191 | 3.191 | 3.191 |
| K2 | 2.995 | 2.995 | 2.995 | 2.995 |
| K3 | 2.998 | 2.876 | 2.876 | 2.876 |
| K4 | 2.953 | 2.813 | 2.813 | 2.813 |
| R  | 0.017 | 0.094 | 0.094 | 0.094 |

Note:  $K_n$  represents the average experimental result at the  $n$ th level of the factor, and  $R$  is the range.

Table 4 presents the results of the warpage deformation range analysis, examining the experimental means ( $K_n$ ) and ranges ( $R$ ) for factors A, B, C, and D at different levels. For factor A,  $K_1=2.928$ ,  $K_2=2.995$ ,  $K_3=2.998$ ,  $K_4=2.953$ , with a range  $R=0.017$ , indicating that the variation in the experimental means across different levels is small, and the range is only 0.017, suggesting that factor A has a weak influence on warpage deformation. For factor B,  $K_1=3.191$ ,  $K_2=2.995$ ,  $K_3=2.876$ ,  $K_4=2.813$ , with a range  $R=0.094$ , indicating a larger variation in the experimental means across different levels, and the range is 0.094, suggesting that factor B has a more significant influence on warpage deformation. For factor C,  $K_1=3.191$ ,  $K_2=2.995$ ,  $K_3=2.876$ ,  $K_4=2.813$ , with a range  $R=0.094$ , showing the same variation in experimental means as factor B, and the range is 0.094, suggesting that factor C also has a significant influence on warpage

deformation. For factor D,  $K1=3.191$ ,  $K2=2.995$ ,  $K3=2.876$ ,  $K4=2.813$ , with a range  $R=0.094$ , indicating the same variation in experimental means as factors B and C, and the range is 0.094, suggesting that factor D also has a significant influence on warpage deformation. In summary, factors B, C, and D have a more significant impact on warpage deformation, while factor A has a weaker influence.

Using Matlab software and the data from Table 4, the influence trends of each process factor at different levels on the deformation are plotted, as shown in Figure 7.

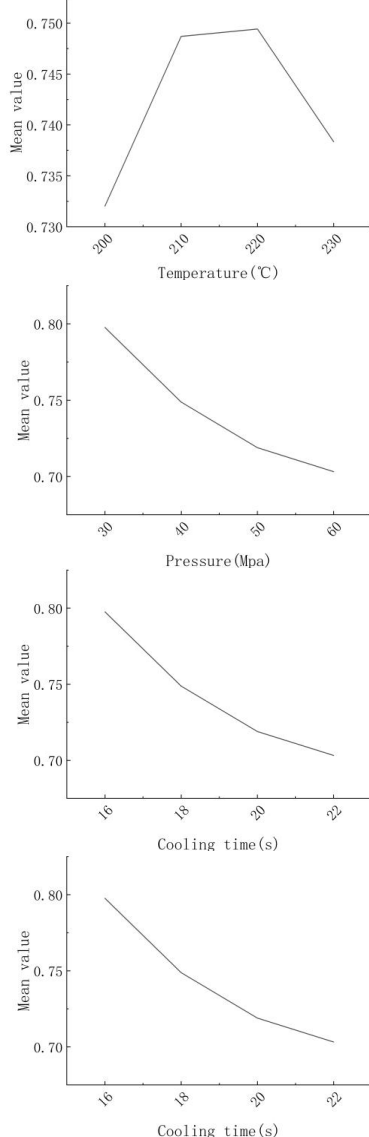


**Figure 7. Influence Trend of Each Factor on Warpage Deformation**

As shown in Figure 7, with the increase in melt temperature, the warpage deformation initially increases slowly, then gradually decreases. When the melt temperature reaches 200°C, the

warpage deformation reaches its minimum value. This is mainly due to the fact that when the melt temperature exceeds a certain threshold, excessive holding pressure can occur, leading to an increase in warpage deformation. With the increase in holding pressure, holding time, and cooling time, the warpage deformation of the part consistently decreases. The higher the holding pressure, the longer the holding time, and the longer the cooling time, the plastic part remains in a molten state for a longer period during the injection molding process, which helps the molecular chains relax, thereby reducing the internal stress and deformation of the product. The warpage deformation reaches its minimum when the holding pressure is 60 MPa, holding time is 14 s, and cooling time is 22 s. Although warpage deformation shows a negative correlation with holding pressure, holding time, and cooling time, these parameters do not necessarily need to be maximized. Higher values of these parameters would result in longer injection cycles, increasing the production cost of the mold and reducing production efficiency. Based on the above analysis, the optimal parameter combination after orthogonal testing within the suitable process range for the material is A4B4C4D4, where the melt temperature is 200°C, holding pressure is 60 MPa, holding time is 14 s, and cooling time is 22 s.

#### 4.5 Optimization Result Verification Analysis

Based on the optimized process parameters obtained from the Taguchi experiment, Moldflow software was used to perform a simulation analysis on the plastic part. The selected process parameters were: melt temperature of 200°C, holding pressure of 60 MPa, holding time of 14 s, and cooling time of 22 s. The resulting warpage deformation is shown in Figure 8.

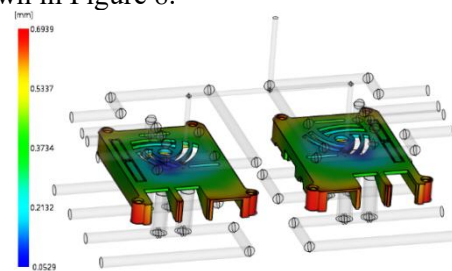


**Figure 8. Warpage Deformation After Process Parameter Optimization**

As shown in Figure 8, the total warpage deformation after optimizing the process parameters is 0.6939 mm, which is smaller than the warpage deformation of all 16 orthogonal experimental trial schemes. This represents a reduction of 0.1576 mm compared to the deformation of 0.8515 mm in the initial scheme, resulting in a decrease of approximately 18.5%. Furthermore, this deformation meets the assembly requirements of the product, with the maximum internal deformation not exceeding 0.7 mm.

## 5. Conclusion

The Taguchi method was used to optimize the process parameters, with orthogonal experiments and range analysis conducted. The results indicate that holding pressure has the greatest influence on warpage deformation. The minimum warpage deformation is achieved when the optimal parameter combination is a melt temperature of 200°C, holding pressure of 60 MPa, holding time of 14 s, and cooling time of 22 s.

The miniature computer casing is a thin-walled plastic part. Therefore, conformal cooling is applied externally, and cooling water channels with baffles are used internally. The analysis results indicate that the cooling system, including the baffle cooling channels and conformal cooling circuits, is well-designed, with the cooling fluid temperature and part temperature staying consistent, demonstrating effective cooling performance.

## Acknowledgments

This study was supported by the Natural Science Foundation of Top Talent of SZTU (grant no. GDRC202408), Shenzhen Postdoctoral Research Funding Project (2023-05-05).

## References

- [1].Hyie K M, Budin S, Wahab M. Effect of injection moulding parameters in reducing the shrinkage of polypropylene product using Taguchi analysis[C]//IOP Conference Series: Materials Science and Engineering. IOP Publishing, 2019, 505(1): 012060.
- [2].Wang B, Cai A. Influence of mold design and injection parameters on warpage deformation of thin-walled plastic parts[J]. Polimery, 2021, 66(5): 283-292.
- [3].Zhang J, Yin X, Liu F, et al. The simulation of the warpage rule of the thin-walled part of polypropylene composite based on the coupling effect of mold deformation and injection molding process[J]. Science and Engineering of Composite Materials, 2018, 25(3): 593-601.
- [4].Hamdi A. Assessing the suitability of various grades of polypropylene for injection molding through flow-length measurements[J]. Korea-Australia Rheology Journal, 2024, 36(1): 33-43.
- [5].Usman Jan Q M, Habib T, Noor S, et al. Multi response optimization of injection moulding process parameters of polystyrene and polypropylene to minimize surface roughness and shrinkage's using integrated approach of S/N ratio and composite desirability function[J]. Cogent Engineering, 2020, 7(1): 1781424.
- [6].Li X, Wei Q, Li J, et al. Numerical simulation on crystallization-induced warpage of injection-molded PP/EPDM part[J]. Journal of Polymer Research, 2019, 26: 1-11.
- [7].Willerer T, Brinkmann T, Drechsler K. Development and Application of a Cooling Rate Dependent PVT Model for Injection Molding Simulation of Semi Crystalline Thermoplastics[J]. Polymers, 2024, 16(22): 3194.
- [8].Kumar S, Singh A K. Volumetric shrinkage estimation of benchmark parts developed by rapid tooling mold insert[J]. Sādhanā, 2020, 45: 1-9.
- [9].Lin W C, Fan F Y, Huang C F, et al. Analysis of the warpage phenomenon of micro-sized parts with precision injection molding by experiment, numerical simulation, and grey theory[J]. Polymers, 2022, 14(9): 1845.
- [10].Dastjerdi M, Dastjerdi A M A, Dastjerdi P M A, et al. Feasibility of developing green water batteries based on poly-lactic acid and polybutylene succinate: A computational study on groasis waterboxx technology[J]. Materials Today Communications, 2023, 36: 106537.
- [11].Saedon J B, Azlan M Z, Adenan M S, et al. CAE analysis for disposable mouth mirror based on autodesk moldflow plastic insight[C]//IOP Conference Series: Materials Science and Engineering. IOP Publishing, 2020, 834(1): 012060.
- [12].Tsai H H, Wu S J, Liu J W, et al.

- Filling-balance-oriented parameters for multi-cavity molds in polyvinyl chloride injection molding[J]. *Polymers*, 2022, 14(17): 3483.
- [13]. Abdul R, Guo G, Chen J C, et al. Shrinkage prediction of injection molded high density polyethylene parts with taguchi/artificial neural network hybrid experimental design[J]. *International Journal on Interactive Design and Manufacturing (IJIDeM)*, 2020, 14: 345-357.
- [14]. Kuo C F J, Su T L, Li Y C. Construction and analysis in combining the Taguchi method and the back propagation neural network in the PEEK injection molding process[J]. *Polymer-Plastics Technology and Engineering*, 2007, 46(9): 841-848.
- [15]. Shen C, Wang L, Cao W, et al. Investigation of the effect of molding variables on sink marks of plastic injection molded parts using Taguchi DOE technique[J]. *Polymer-Plastics Technology and Engineering*, 2007, 46(3): 219-225.